Identification of amino acid residues important in the cyclization reactions of chalcone and stilbene synthases

Dae-Yeon SUH*, Kazuki FUKUMA*, Junichi KAGAMI*, Yasuyo YAMAZAKI*, Masaaki SHIBUYA†, Yutaka EBIZUKA† and Ushio SANKAWA*[1]

*Faculty of Pharmaceutical Sciences, Toyama Medical and Pharmaceutical University, 2630 Sugitani, Toyama 930-0194, Japan, and †Graduate School of Pharmaceutical Sciences, The University of Tokyo, 7-3-1 Hongo, Bunkyo-ku, Tokyo 113-0033, Japan

Chalcone synthase (CHS) and stilbene synthase (STS) catalyse condensation reactions of *p*-coumaroyl-CoA and three C_2 units from malonyl-CoA up to a common tetraketide intermediate but then catalyse different cyclization reactions to produce naringenin chalcone and resveratrol respectively. On the basis of sequence alignment with other condensing enzymes including 3-ketoacyl-(acyl carrier protein) synthases of polyketide and fatty-acid synthases, site-directed mutagenesis was performed on the active-site G^{372}FGPG loops in CHS and STS. The CHS-P375G mutant showed a 6-fold decrease in overall condensing activity with selectively increased production of *p*-coumaroyltriacetic acid lactone (CTAL, the derailment product of the tetraketide intermediate). Meanwhile, resveratrol production by STS-P^{375}G strongly decreased to give various products in the order CTAL > resveratrol ≈ bisnoryangonin > naringenin. As a result, naringenin production (cross-reaction) by STS-P^{375}G was close to 30% of resveratrol production. Both G^{374}L mutants of CHS and STS showed no condensing activity with residual malonyl-CoA decarboxylase activity. These results suggested that the G^{372}FGPG loop in CHS and STS contribute to a determination of the outcome during cyclization reactions by serving as a part of the active-site scaffold on which the stereochemistry of cyclization is performed. These observations provide the first biochemical indication that cyclization reactions are modulated by active-site geometry. The implications for the evolutionary relationship of these enzymes are also discussed.

Key words: active-site geometry, condensing enzymes, cross-reaction.

INTRODUCTION

Chalcone synthase (CHS, EC 2.3.1.74), which is ubiquitous in plants, catalyses the first committed reaction of flavonoid and isoflavone biosynthesis. Stilbene synthase (STS, EC 2.3.1.95), found in a limited number of unrelated plants, catalyses the biosynthesis of the backbone of phytoalexin stilbenes [1,2]. Both enzymes share common features in structure and function. They are homodimers of approx. 43 kDa subunits and catalyse decarboxylative Claisen condensation of a phenylpropanoid CoA-ester (e.g. *p*-coumaroyl-CoA) and three C_2 units from malonyl-CoA, leading to a common linear tetraketide intermediate (Figure 1). However, the ensuing cyclization reactions in CHS and STS are different. In CHS, acylation involving carbons 6 and 1 gives rise to chalcone. In STS, cyclization involving carbons 2 and 7 is accompanied by the removal of the terminal carboxy group, yielding stilbene. The amino acid sequence similarity between these two enzymes is more than 65%. Higher similarity between CHS and STS from related plants than between CHSs and STSs led to a suggestion that STSs have evolved from CHSs several times independently [3]. CHS and STS are representative members of the CHS enzyme superfamily, which now includes *Gerbera hybrida* 2-pyrone synthase [4], *Humulus lupulus* phlorisovalerophenone synthase [5] and *Hydrangea macrophylla p*-coumaroyltriacetic acid synthase [6]. Recent studies on the bacterial genes encoding the CHS-like proteins phlD from *Pseudomonas fluorescens* [7] and rppA from *Streptomyces griseus* [8] expand the superfamily into the realm of micro-organisms. The phlD enzyme is proposed to catalyse condensation of acetoacetyl-CoA with two molecules of malonyl-CoA and the CHS-type cyclization to give a phloroglucinol, whereas the rppA protein catalyses four steps of condensation with malonyl-CoA as starter and extender units and a decarboxylative cyclization to produce a tetrahydroxynaphthalene. These newly discovered CHS-like enzymes demonstrate a broader diversity in the CHS superfamily with regard to starter CoA and the number of condensation reactions and biological origin than previously realized.

On the basis of common chemistry (decarboxylative condensation) and the reported local similarity in CHS and other condensing enzymes [9], particularly in the C-terminal sequences of CHS and 3-ketoacyl-(acyl carrier protein) synthases (KASs) [10,11], we reasoned that the active-site structures of CHS and STS and other condensing enzymes might share common features. To address this hypothesis, we first predicted on a computer (with PREDATOR) [12] the secondary structures of CHS and STS and aligned the C-end regions of CHS and STS with those of other condensing enzymes, including *Escherichia coli* KAS II [13], in such a way as to optimize matches of the secondary structures. As shown in Figure 2, a similarity in the secondary structure organization and the locations of highly conserved amino acids was recognized. The strictly conserved His-303, Asn-336 and Pro-375 of *Pueraria lobata* CHS and *Arachis hypogaea* STS are aligned with His-303, His-340 and Phe-400 of *E. coli* KAS II respectively, all of which are located at the active site of KAS II [13]. Indeed, the recently determined three-dimensional structure of alfalfa (*Medicago sativa*) CHS (PDB accession no. 1BI5) [14] revealed that these amino acid

Abbreviations used: BNY, bisnoryangonin; CHS, chalcone synthase; CTAL, *p*-coumaroyltriacetic acid lactone; KAS, 3-ketoacyl-(acyl carrier protein) synthase; LC/APCIMS, liquid chromatography/atmospheric-pressure chemical-ionization MS; RP-TLC, reverse-phase TLC; STS, stilbene synthase; Trx, thioredoxin.

[1] To whom correspondence should be addressed. Present address: International Traditional Medicine Research Center, Toyama International Health Complex, 151 Tomosugi, Toyama 939-8224, Japan (e-mail sankawa@toyama-prof-ihc.or.jp).

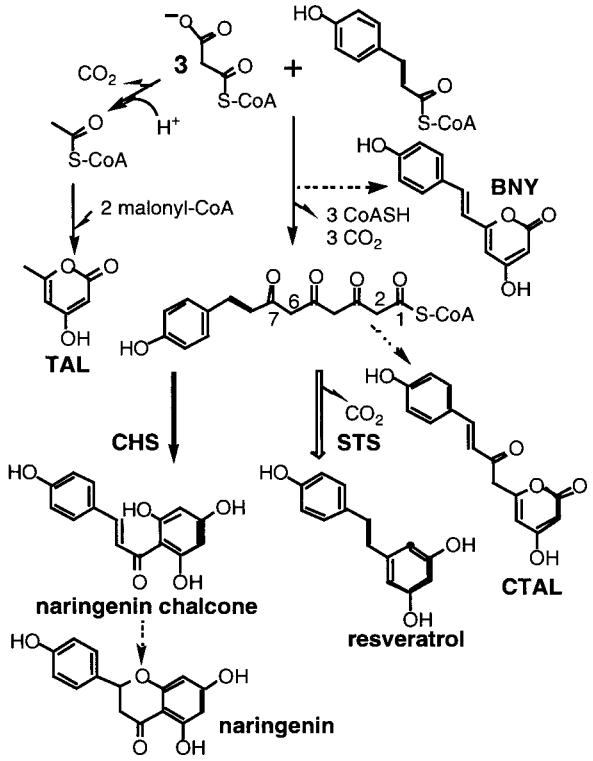

Figure 1 Reactions catalysed by chalcone and stilbene synthases

Reactions leading to the by-products BNY, CTAL and triacetic acid lactone (TAL) are also shown. Chemical bonds originating from the C_2 units of malonyl-CoA are indicated by thick lines. Naringenin chalcone is chemically converted into naringenin under the reaction conditions used. In plant cells, chalcone isomerase catalyses the stereospecific conversion of naringenin chalcone into (−)(2*S*)-naringenin.

residues, along with Phe-215, largely define the active site of alfalfa CHS, validating the alignment presented in Figure 2. A prominent feature found in Figure 2 is that the G^{372}FGPG loop in the CHS superfamily enzymes contains a strictly conserved proline residue, unlike the corresponding flexible loop of S^{397}FGFG in KAS II [13]. This Pro-375 residue, which should provide some rigidity and unique configuration in this loop, was mutated to Gly to investigate the functional role of the G^{372}FGPG loop in CHS and STS. In addition, Gly-374 was changed to Leu in an attempt to introduce a bulky side chain in the loop.

EXPERIMENTAL

Site-directed mutagenesis

Wild-type and mutant CHS and STS were expressed as thioredoxin–His-tagged fusion proteins (Trx-CHS and Trx-STS) for improved solubility and easy purification with pET-32a(+) (Novagen) as expression vector. The full-length cDNA species encoding *P. lobata* CHS and *A. hypogaea* STS were rescued by sequential *Nco*I/*Bam*HI digestions from pET3d-CHS and pET3d-STS [15]. The resulting DNA fragments were sticky-end ligated into *Nco*I/*Bam*HI-digested dephosphorylated pET-32a, yielding pET-CHS and pET-STS. Mutagenesis was performed with the PCR megaprimer method [16] with pET-CHS and pET-STS as templates. The forward flanking primers were 5′-GACAAGGCC*ATGG*TGAGCGTA-3′ (the start codon is in italics and the *Nco*I site is underlined) for Trx-CHS and 5′-GACAAGGCC*ATGG*TGTCTG-3′ for Trx-STS. The reverse primers were 5′-TGTGGATCCAAACTCCAGCAAGT-3′ (the *Bam*HI site is underlined) for Trx-CHS and 5′-TTCGGATCC-CCCGTATTATA-3′ for Trx-STS. Because of high nucleotide sequence similarity in CHS and STS, a single mutagenic primer was used to create mutants of both enzymes. The mutagenic primer for the G^{374}L mutants was 5′-GGTTTT**CTT**CCTGGA-CTTACTATTG-3′ (the mutated residue is in bold) and the primer for the P^{375}G mutants was 5′-GGTTTTGGA**GGT**GGT-CTTACTATTG-3′. After first PCR with the mutagenic primer and the reverse flanking primer, a second PCR was performed with the forward flanking primer and the first PCR products (megaprimer), giving full-length DNA fragment containing the desired mutation. High-fidelity *Ex Taq* DNA polymerase (Takara, Japan) was used in the PCR. The mutations were confirmed by DNA sequence analysis with the flanking primers and the Dye Terminator Cycle Sequencing kit (Applied Biosystems).

Protein expression and purification

Wild-type and mutant enzymes were expressed in *E. coli* AD494-(DE3)pLysS (Novagen). After an induction period of 20 h at 25 °C (10 h for the G^{374}L mutants), the soluble fraction obtained in accordance with the manufacturer's recommendations was applied to a column of Ni^{2+}-iminodiacetic acid–Sepharose (Chelating Sepharose Fast Flow; Pharmacia) equilibrated with buffer A [20 mM sodium phosphate buffer (pH 7.4)/300 mM NaCl/10 % (v/v) glycerol/0.1 % (v/v) Triton X-100/10 mM imidazole/5 mM 2-mercaptoethanol]. After the column had been washed with 80 mM imidazole in buffer A, the fusion proteins were eluted with 250 mM imidazole in buffer A and stored in buffer B [100 mM potassium phosphate buffer (pH 7.2)/10 % (v/v) glycerol/0.1 % (v/v) Triton X-100/1 mM dithiothreitol]. Protein concentration was determined with Bio-Rad's adaptation of the Bradford dye assay [17] with Trx-CHS as standard.

Enzyme assay

The condensing activity of the enzyme was determined as described previously [15] except that the reaction was performed in buffer B and terminated by acidification to pH 4 with 1 M HCl. Derailment products, bisnoryangonin (BNY) and *p*-coumaroyltriacetic acid lactone (CTAL), were identified from their R_F values [BNY, R_F 0.4; CTAL, R_F 0.6 in reverse-phase C_{18} TLC with methanol/water/acetic acid (60:40:1, by vol.) as solvent] [15]. The detection method consisted of acidification, extraction with ethyl acetate and reverse-phase TLC (RP-TLC) of the radiolabelled products. This permitted the simultaneous quantification of all the products. Chemical transformation of naringenin chalcone to naringenin (Figure 1) was complete under the reaction conditions used; no appreciable amounts of chalcone were detected.

Malonyl-CoA decarboxylase activity was determined by following the formation of acetyl-CoA [4]. At the end of the enzyme reaction for 20 min at 37 °C in 0.1 M Hepes, pH 7.0, with 100 μM [2-^{14}C]malonyl-CoA, a 10–20 μl portion of the aqueous phase was analysed on a silica 60 TLC plate (catalogue no. 1.11798; Merck) with propan-2-ol/water/25 % (v/v) ammonia (80:5:15, by vol.) as solvent, permitting the separation of acetyl-CoA (R_F 0.6) from remaining malonyl-CoA (R_F 0.25). The specific enzyme activity was expressed in pmol of product produced/s per mg (pkat/mg).

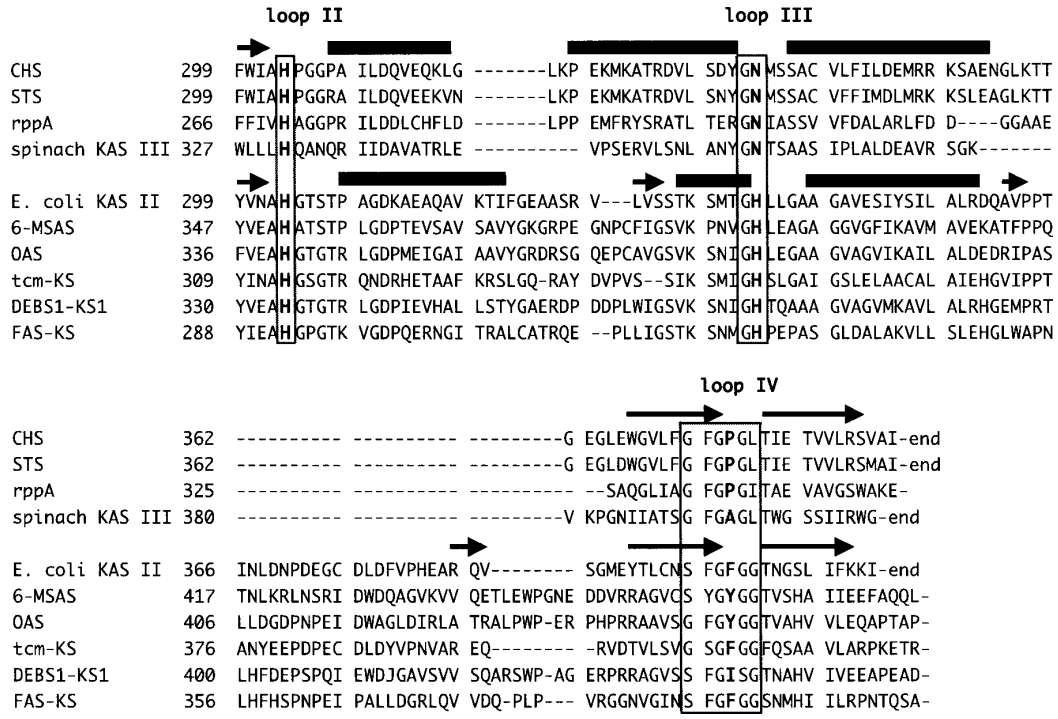

Figure 2 Alignment of amino acid sequences of chalcone and stilbene synthases with other condensing enzymes

Amino acid sequences of the C-terminal ends of CHS and STS were aligned with the corresponding regions of other condensing enzymes by comparing secondary structures (α-helices indicated by thick bars and β-sheets by arrows) of CHS [14] and *E. coli* KAS II [13]. Of the four loops that largely make up the active site of CHS, loop I containing the nucleophilic reaction centre Cys-164 is not shown. The abbreviations and GenBank accession numbers are as follows: CHS, *P. lobata* CHS (D10223); STS, *A. hypogaea* stilbene synthase (AB027606); *rppA*, *Streptomyces griseus* gene similar to CHS (AB018074); spinach KAS III, *Spinacia oleracea* KAS III (CAA80452); *E. coli* KAS II, *E. coli* KAS II (P39434); 6-MSAS, *Aspergillus terreus* 3-ketoacyl synthase domain of 6-methylsalicyclic acid synthase (D85860); OAS, *Streptomyces viridochromogenes* 3-ketoacyl synthase domain of orsellinic acid synthase (CAA72713); tcm-KS, *Streptomyces glaucescens* tetracenomycin polyketide synthase condensing enzyme (M80674); DEBS1-KS1, *Saccharopolyspora erythraea* 6-deoxyerythronolide B synthase condensing domain (module 1) (S13595); FAS-KS, *Homo sapiens* 3-ketoacyl synthase domain of fatty-acid synthase (P49327).

Steady-state kinetic analysis

All kinetic experiments were performed in 0.1 M Hepes at pH 7.0. The K_m (app) values for *p*-coumaroyl-CoA in the condensing reaction were determined at a malonyl-CoA concentration of 10 μM; those for malonyl-CoA were determined at 100 μM *p*-coumaroyl-CoA. Under these conditions, the production of triacetic acid lactone, an aberrant by-product formed from two malonyl-CoA molecules and acetyl-CoA that is derived from malonyl-CoA decarboxylation *in situ* (Figure 1), was minimal, permitting reliable determination of the K_m (app) values for naringenin and resveratrol formation. The reactions were performed with 2 μg of the wild-type enzymes and 10 μg of the mutants at 37 °C for 20 min, then analysed by TLC as described previously [15]. The K_m (app) values for malonyl-CoA in malonyl-CoA decarboxylation were determined in the absence of *p*-coumaroyl-CoA. The reaction mixture (50 μl) contained enzyme (1 μg of wild-type enzyme and 5 μg of mutant) and various concentrations of malonyl-CoA. After 20 min at 37 °C, 5 μl of 1 M HCl was added to terminate the reaction. A 10 μl aliquot of the reaction mixture was applied directly to a silica 60 TLC plate to quantify acetyl-CoA formation. For each experiment, five substrate concentrations covering the range 0.2–5 K_m (app) were employed. The data of v against [S] were fitted to the Michaelis–Menten equation; the V_{max} and K_m (app) values were obtained with a non-linear regression program (SigmaPlot; Jandel Scientific).

Identification of the reaction products of the P[375]G mutant of STS by LC-MS

Reaction products produced by STS-P[375]G (10 mg, 2 pkat/mg for resveratrol production) were identified by liquid chromatography/atmospheric-pressure chemical-ionization MS (LC/APCIMS) as described previously [15], except that substrate concentrations of 0.1 mM *p*-coumaroyl-CoA and 0.1 mM malonyl-CoA were used.

RESULTS

Expression and purification

The enzymes were expressed as Trx fusion proteins and they were joined with the Trx protein at their N-ends via a linker containing the His_6 tag and an enterokinase cleavage site. These Trx fusion proteins are hereafter referred to as CHS and STS unless otherwise noted. The His_6 tag enabled us to obtain the wild-type enzyme and the P[375]G mutants in apparent homogeneity after a single purification step with Ni^{2+}-chelation chromatography (Figure 3A). Mutant enzymes were purified under conditions that were essentially identical with those used for the wild-type enzymes. The Pro-375 → Gly mutation in both CHS and STS apparently disturbed the folding process so that most of the expressed P[375]G mutants were recovered in an insoluble fraction as inclusion bodies. This resulted in an approx. 4-fold decrease in

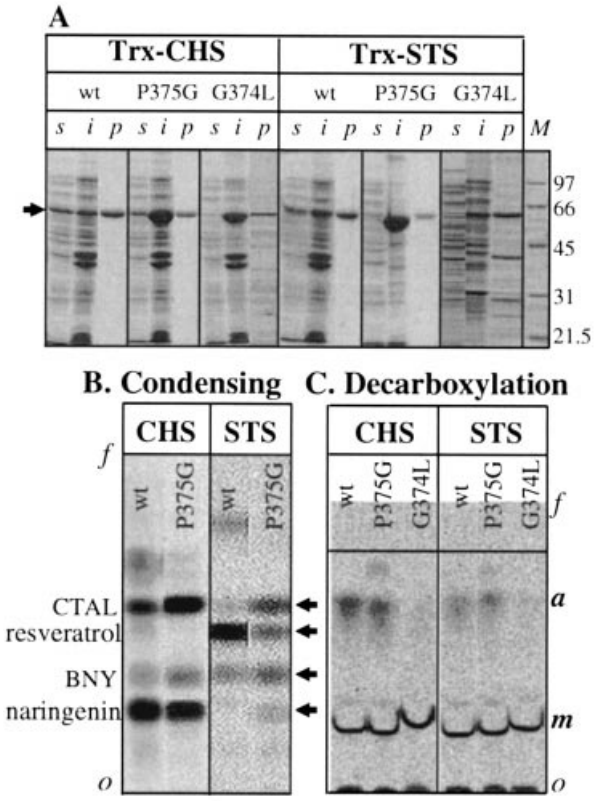

Figure 3 SDS/PAGE (A) and radio-TLC (B, C) of the wild-type and mutant chalcone and stilbene synthases

(**A**) Soluble (s) and insoluble (i) *E. coli* extracts and purified (p) Trx–CHS and Trx–STS enzymes (60 kDa, arrow) are shown. Proteins were separated on 12% (w/v) polyacrylamide mini-slab gels under reducing conditions, followed by staining with Coomassie Brilliant Blue R250. Lane M, molecular mass markers (molecular masses are shown in kDa at the right). (**B**, **C**) Radio-TLC of CHS and STS reaction products. Condensing activities of wild-type and $P^{375}G$ mutants of CHS and STS (**B**) were determined with *p*-coumaroyl-CoA and [2-^{14}C]malonyl-CoA as substrates. The cyclization products (naringenin and resveratrol) as well as derailment products (BNY and CTAL) were separated and quantified by using reversed-phase (C_{18}) TLC and an Imaging Plate Analyzer (BAS2000; Fuji). The products were identified by using authentic samples or by a comparison of their known R_F values [15]. C. Malonyl-CoA decarboxylation (acetyl-CoA formation) activity (**C**) was assayed with [2-^{14}C]malonyl-CoA as a sole substrate. Acetyl-CoA (a) and malonyl-CoA (m) were separated on a silica 60 TLC plate and identified by comparing their R_F values [4]. The reactions were performed with 1 μg of the wild-type enzyme, 5 μg of the $P^{375}G$ mutant enzyme or 15 μg of the $G^{374}L$ mutant enzyme. o, TLC origin; f, solvent front.

the yields of the purified mutants in comparison with the wild-type enzymes (Table 1). The Gly-374 → Leu mutation exhibited more adverse effects during expression, especially in the STS-$G^{374}L$ mutant. A time-course study nevertheless revealed a peak in expression level at 10–12 h after induction as judged by SDS/PAGE (results not shown). Hence both the $G^{374}L$ mutants were harvested after 10 h induction at 25 °C. Owing to lower expression levels and solubilities, the $G^{374}L$ mutants were only partly purified by Ni^{2+}-chelation chromatography (Figure 3A).

Enzyme activity and product profile of mutant enzymes

Purified enzymes were analysed for their ability to catalyse both condensing and malonyl-CoA decarboxylation reactions. Wild-type native CHS and STS enzymes recovered by cleavage of the Trx-fusion enzymes with enterokinase (Stratagene) showed product profiles and specific activities that were virtually identical with those of the fusion enzymes. This indicates that the Trx polypeptide in the fusion protein does not interfere with the CHS and STS reactions. However, the native enzymes were less stable; the Trx-fusion enzymes were therefore used in this study.

During the CHS and STS reactions *in vitro*, BNY and CTAL are also produced as derailment products by hydrolysis of the growing chain at the stage of triketide and tetraketide respectively (Figures 1 and 3B) [6,15,18]. The detection method (acidification of reaction mixture followed by extraction and RP-TLC analysis) was chosen to follow both the production of not only the final products but also the derailment products so as to assess the mutational effects on the active site. CHS and STS also catalyse malonyl-CoA decarboxylation and CO_2 exchange in both the presence and the absence of *p*-coumaroyl-CoA [19,20]. The decarboxylation of malonyl-CoA initially produces an acetyl-CoA carbanion, which is subsequently protonated to acetyl-CoA (Figure 1). In the present study, acetyl-CoA formation was followed, to measure malonyl-CoA decarboxylation activity in the absence of *p*-coumaroyl-CoA (Figure 3C).

When Pro-375 was mutated to Gly in CHS, specific activities calculated for the condensation reaction (total C_2 units condensed for all the products/s per mg of protein) and malonyl-CoA decarboxylation decreased 5.9-fold and 6.8-fold respectively (Table 1). However, a smaller decrease in V_{max} values for condensation (3.1-fold) and for decarboxylation (1.6-fold) indicated that Pro-375 has a limited role in the early step of malonyl-CoA decarboxylation (Table 2) and that the larger differences in specific activities were due partly to different degrees of purity. More interestingly, the product profile of CHS-$P^{375}G$ was also changed. Whereas the ratio of CTAL to naringenin produced by the wild-type CHS was less than 0.4, the same ratio in the CHS-$P^{375}G$-catalysed reaction increased to nearly 0.9 under identical reaction conditions (Figure 3B). In contrast, BNY production remained relatively constant (5–7% of total condensations) in the wild-type CHS and CHS-$P^{375}G$. These results indicated that selectively increased CTAL production by the $P^{375}G$ mutant was not simply due to a 'loosening up' of the active site caused by increased flexibility in the loop. This 'loosening up' effect would have resulted in an increased access of solvent water to the growing intermediates, leading to an increased production of both derailment products. Rather, it seemed more likely that the change in the active-site configuration of the CHS-$P^{375}G$ mutant impeded proper CHS-type folding of the enzyme-bound tetraketide intermediate, which should eventually be hydrolysed by solvent water. Once hydrolysed, the resulting free tetraketide could no longer undergo the CHS-type cyclization because the cyclization (intramolecular Claisen condensation) requires an activated carbonyl carbon (Figure 1). As a result, the free tetraketide probably diffuses out of the active site and undergoes spontaneous lactonization to give CTAL.

The K_m (app) and V_{max} values for the wild-type STS and STS-$P^{375}G$ mutant were not significantly different, indicating that the Pro-375 → Gly mutation did not significantly affect the malonyl-CoA binding and decarboxylation reaction of STS. However, the same mutation had a drastic effect on the product profile. Whereas the product profile in the wild-type STS reaction was resveratrol ≫ CTAL ≈ BNY > naringenin, it changed to CTAL > resveratrol ≈ BNY > naringenin in the STS-$P^{375}G$ reaction (Table 1 and Figure 3B). Clearly, the ability of this mutant to catalyse the STS-type cyclization to produce resveratrol was greatly impaired. The concurrent increase in production of BNY and CTAL suggested that, in contrast with CHS-$P^{375}G$, 'loosening up' of the active site in STS-$P^{375}G$ had a

Table 1 Expression, product profile and enzyme activity of the wild-type and mutant chalcone and stilbene synthases

Results are means ± S.D. ($n = 3$–6). Yields are those of purified enzymes obtained after a Ni^{2+}-chelation chromatography step. For determining the product profiles and measuring the specific activity of the condensing reaction, the reaction was performed in 0.1 M potassium phosphate, pH 7.2, containing 10% (v/v) glycerol, 0.1% (v/v) Triton X-100 and 1 mM dithiothreitol with 0.1 mM *p*-coumaroyl-CoA and 16.8 μM [2-^{14}C]malonyl-CoA as substrates. Specific activity is defined as pmol of C_2 units condensed/s per mg of protein (pkat/mg). For measuring the specific activity of the malonyl-CoA decarboxylation, the reaction was performed in 0.1 M Hepes, pH 7.0, with 100 μM [2-^{14}C]malonyl-CoA as a sole substrate. The amounts of enzymes added to the reaction were: wild-type enzymes, 1 μg; P375G mutants, 5 μg; G374L mutants, 15 μg. Specific activity is defined as pmol of acetyl-CoA produced/s per mg of protein (pkat/mg). 'Inactive' signifies that even with 30 μg of partly purified mutant enzyme (Figure 3), the amounts of any products were below the detection limit.

Enzyme	Variant	Yield (mg/100 ml of culture)	Product profile (mol%)				Specific activity (pkat/mg)	
			Naringenin	CTAL	BNY	Resveratrol	Condensing reaction	Malonyl-CoA decarboxylation
CHS	Wild-type	8.2 ± 2.9	68 ± 7.5	24 ± 4.2	5.3 ± 2.4	3.0 ± 1.7	220 ± 32	390 ± 39
	G374L	0.14 ± 0.014					Inactive	0.71 ± 0.71
	P375G	2.4 ± 1.9	48 ± 6.5	43 ± 3.6	6.7 ± 3.1	2.5 ± 1.5	37 ± 1.6	57 ± 16
STS	Wild-type	8.0 ± 2.2	1.7 ± 0.41	10 ± 7.0	8.6 ± 3.7	79 ± 8.8	280 ± 80	170 ± 35
	G374L	0.15 ± 0.028					Inactive	1.2 ± 1.0
	P375G	1.8 ± 1.2	7.3 ± 1.0	42 ± 5.2	24 ± 4.3	27 ± 4.3	60 ± 20	39 ± 3.8

Table 2 Kinetic parameters of the wild-type and mutant chalcone and stilbene synthases

Results are means ± S.D. ($n = 3$). Under the heading 'Condensing reaction' are shown K_m(app) and V_{max} values for naringenin production by CHS and for resveratrol production by STS.

Enzyme	Variant	Condensing reaction			Malonyl-CoA decarboxylation	
		K_m (app) (μM)		V_{max} (pmol/s per ml)	K_m (app) (μM)	V_{max} (pmol/s per ml)
		p-Coumaroyl-CoA	Malonyl-CoA			
CHS	Wild-type	50 ± 7.1	3.0 ± 1.2	0.46 ± 0.27	49 ± 6.4	12 ± 1.2
	P375G	44 ± 2.8	2.5 ± 0.71	0.15 ± 0.04	23 ± 2.9	7.6 ± 1.4
STS	Wild-type	22 ± 5.7	2.0 ± 0.89	0.53 ± 0.23	31 ± 11	4.7 ± 1.0
	P375G	16 ± 0.71	0.89 ± 0.10	0.13 ± 0.06	22 ± 5.5	5.2 ± 0.25

major role. Further, STS-P^{375}G exhibited an increased cross-reaction [15] of up to 30%. That is, the mutant catalysed almost one CHS-type cyclization for every three STS-type cyclization reactions. It should be noted that the increased cross-reaction cannot be attributed solely to the decreased production of resveratrol because the specific activity for naringenin production by STS-P^{375}G (1.6 ± 0.60 pkat/mg, mean ± S.D.) remained similar to that of the wild-type enzyme (1.6 ± 0.41 pkat/mg) in spite of the 4.7-fold decrease in condensing ability and the 4.4-fold decrease in malonyl-CoA decarboxylation activity (Table 1). This unexpected result could best be explained by the fact that different cyclization reactions in CHS and STS are indeed controlled by differences in the active-site geometry, which determines the way in which the linear intermediate folds before cyclization [14,21]. It is therefore proposed that the active sites of CHS and STS are configured to favour one type of spatial folding of the intermediate. The P^{375}G mutation alters the STS active site to allow both types of folding to occur partly by 'loosening up' (see the Discussion section).

As a way of assessing whether the mutant retained the conformational integrity of the wild-type enzyme, kinetic parameters of the wild-type and mutant enzymes were compared. As summarized in Table 2, the Pro-375 → Gly mutation in CHS and STS had a limited effect on the K_m (app) values for both substrates, suggesting that the mutants retained the wild-type tertiary structures. The identity of the products formed by STS-P^{375}G was confirmed by LC-APCIMS analysis in positive-ion mode. The results were in complete agreement with earlier reports [6,15]: BNY, MS m/z 231 $[M + H]^+$; CTAL, MS m/z 273 $[M + H]^+$; resveratrol, MS m/z 229 $[M + H]^+$, MS–MS (precursor ion at m/z 229) m/z (rel. %) 211 (50), 135 (100), 119 (17), 107 (18); naringenin, MS m/z 273 $[M + H]^+$, MS–MS (precursor ion at m/z 273) m/z (rel. %) 171 (13), 153 (76), 147 (100).

No condensing activity was detected with the G^{374}L mutants of CHS and STS, even after larger amounts of proteins were added to the reaction. Some residual malonyl-CoA activities were detected but they were less than 1% of the corresponding wild-type activities. Because of the lower expression and solubility of the G^{374}L mutants, the possibility cannot be excluded that the almost complete loss of the enzyme activity is due to minimal amounts of functionally folded enzymes. However, considering the fact that partly purified preparations contained the mutants as the major protein (Figure 3A), it seems more likely that the loss of activity was due either to the blocking of active sites by the bulky side chain of Leu or to the impaired flexibility of the loop.

DISCUSSION

It is generally accepted that CHS and STS catalyse the synthesis of a linear tetraketide intermediate by means of common chemistry and a common set of catalytic amino acid residues. They do differ in subsequent cyclization reactions; however, an understanding of how the enzymes exhibit stereospecific control in different ring formation reactions has proved to be a challenge. To produce different ring systems connecting different sets of carbon atoms, the common tetraketide intermediate must be folded differently in the active sites of CHS and STS (Figure 1). This different folding can in principle be controlled by different active-site geometries. CHS- or STS-specific amino acids that might govern different cyclization reactions have not been identified. Further, the recent report [14] that there is no functional amino acid in the cyclization pocket of CHS to act as a base during cyclization provided support for the notion that different active-site geometries, not different sets of strategically positioned functional residues (bases), control different cyclization reactions in CHS and STS [1,3,21].

Pro-375 in the G^{372}FGPG loop is strictly conserved not only in CHS and STS but in all other members of the CHS superfamily cloned so far. Further, Pro-375 is a characteristic residue uniquely found in the CHS superfamily enzymes and not in any other condensing enzymes (Figure 2). The results obtained in the present study show that the Pro-375 → Gly mutation exhibits different effects in CHS and STS. In CHS, the mutation impeded the ability of the enzyme to catalyse the CHS-type cyclization, resulting in a selectively increased production of the derailment product, CTAL. In contrast, in STS, the mutation resulted in not only a 'loosening up' of the active site to give an increased production of both derailment products, BNY and CTAL, but also a net increase in cross-reaction (naringenin production). These results suggested that, although conserved in the superfamily members, the exact role of the loop in catalysis, especially during cyclization, might differ between the different enzymes in the family.

The X-ray crystal structure of alfalfa CHS showed that the G^{372}FGPG loop makes up a part of the sidewall of the enzyme's active site. The corresponding S^{397}FGFG loop of *E. coli* KAS II is located at the entrance of the active-site pocket and acts primarily as the flexible gate to the active site [13,14]. The results obtained in this study suggest strongly that the G^{372}FGPG loops in CHS and STS contribute to determining the outcome during cyclization reactions by serving as a part of the active-site scaffold on which the stereochemistry of cyclization is performed. This can be realized by providing both van der Waals interactions [14] and physical confinement during intermediate folding. Similar cases, in which an alteration of the active-site geometry by evolution or by site-directed mutagenesis has led to a novel enzyme activity, can be found in the conversion of oleate 12-desaturase into oleate 12-hydroxylase and of 13-lipoxygenase into 9-lipoxygenase [22,23].

However, it should be noted that the chemistry of the STS-type cyclization is more complex than that of the CHS-type cyclization. The STS-type reaction involves hydrolysis, cyclization and decarboxylation, although the order of events is yet to be resolved. A clear understanding of how these enzymes perform different cyclization reactions requires a knowledge of the three-dimensional structures of STS and other members of the family including *p*-coumaroyltriacetic acid synthase, which does not catalyse a cyclization reaction [6].

The local similarity and conservation of the key residues and structural elements between CHS and other condensing enzymes presented here (Figure 2) raises an interesting point about the evolutionary origin of CHS and STS. Enzymes of secondary metabolism have evolved from pre-existing enzymes, ultimately from those involved in primary metabolism. Even though it has been suggested that CHS and STS are evolutionarily connected with the condensing enzymes (KAS) in fatty-acid synthases [24], a lack of overall similarity has prevented this notion from gaining general acceptance [3]. The recent demonstration of functional CHS-like enzymes in micro-organisms [7,8], together with information presented in this study, should provide new insights into understanding this long-standing question. One attractive model is that the ancient CHS, along with other CHS-like enzymes including the bacterial enzymes, diverged from the evolutionary line of other condensing enzymes (KAS in fatty-acid and polyketide synthases) to meet the need for a variety of secondary metabolites including flavonoids. This process could have involved developing a new functional role for the GFGPG loop by mutating a bulky amino acid to a proline residue.

We thank Dr. Jerald C. Hinshaw (University of Utah, Salt Lake City, UT, U.S.A.) for a critical reading of manuscript. We are grateful to the Ministry of Education, Science, Sports and Culture of Japan for Grants-in Aid for Scientific Research (B) (no. 09044212) and (C) (no. 10680564). D.-Y.S. thanks Tokyo Biochemistry Research Foundation for a fellowship (TBRF-98-10).

REFERENCES

1 Schröder, J. (1999) The chalcone/stilbene synthase-type family of condensing enzymes. In Comprehensive Natural Products Chemistry, vol. 1 (Sankawa, U., ed.), pp. 749–771, Elsevier, Amsterdam
2 Schröder, J. (1997) A family of plant-specific polyketide synthases. Facts and predictions. Trends Plant Sci. **2**, 373–378
3 Tropf, S., Lanz, T., Rensing, S. A., Schröder, J. and Schröder, G. (1994) Evidence that stilbene synthases have developed from chalcone synthases several times in the course of evolution. J. Mol. Evol. **38**, 610–618
4 Eckermann, S., Schröder, G., Schmidt, J., Strack, D., Edrada, R. A., Helariutta, Y., Elomaa, P., Kotilainen, M., Kilpeläinen, I., Proksch, P. et al. (1998) New pathway to polyketide in plants. Nature (London) **396**, 387–390
5 Paniego, N. B., Zuurbier, K. W. M., Fung, S.-Y., van der Heijden, R., Scheffer, J. J. C. and Verpoorte, R. (1999) Phlorisovalerophenone synthase, a novel polyketide synthase from hop (*Humulus lupulus* L.) cones. Eur. J. Biochem. **262**, 612–616
6 Akiyama, T., Shibuya, M., Liu, H.-M. and Ebizuka, Y. (1999) *p*-Coumaroyltriacetic acid synthase, a new homologue of chalcone synthase, from *Hydrangea macrophylla* var. *thunbergii*. Eur. J. Biochem. **263**, 834–839
7 Bangera, M. G. and Thomashow, L. S. (1999) Identification and characterization of a gene cluster for synthesis of the polyketide antibiotic 2,4-diacetylphloroglucinol from *Pseudomonas fluorescence* Q2–87. J. Bacteriol. **181**, 3155–3163
8 Funa, N., Ohnishi, Y., Fujii, I., Shibuya, M., Ebizuka, Y. and Horinouchi, S. (1999) A new pathway for polyketide synthesis in microorganisms. Nature (London) **400**, 897–899
9 Siggaard-Andersen, M. (1993) Conserved residues in condensing enzyme domains of fatty acid synthases and related sequences. Protein Seq. Data Anal. **5**, 325–335
10 Tai, H. and Jaworski, J. G. (1993) 3-Ketoacyl-acyl carrier protein synthase III from spinach (*Spinacia oleracea*) is not similar to other condensing enzymes of fatty acid synthase. Plant Physiol. **103**, 1361–1367
11 Tsay, J.-T., Oh, W., Larson, T. J., Jackowski, S. and Rock, C. O. (1992) Isolation and characterization of the β-ketoacyl-acyl carrier protein synthase III gene (*fabH*) from *Escherichia coli* K-12. J. Biol. Chem. **267**, 6807–6814
12 Frishman, D. and Argos, P. (1997) Seventy-five percent accuracy in protein secondary structure prediction. Proteins **27**, 329–335
13 Huang, W., Jia, J., Edwards, P., Dehesh, K., Schneider, G. and Lindqvist, Y. (1998) Crystal structure of β-ketoacyl-acyl carrier protein synthase II from *E. coli* reveals the molecular architecture of condensing enzymes. EMBO J. **17**, 1183–1191
14 Ferrer, J.-L., Jez, J. M., Bowman, M. E., Dixon, R. A. and Noel, J. P. (1999) Structure of chalcone synthase and the molecular basis of plant polyketide biosynthesis. Nat. Struct. Biol. **6**, 775–784
15 Yamaguchi, T., Kurosaki, F., Suh, D.-Y., Sankawa, U., Nishioka, M., Akiyama,T., Shibuya, M. and Ebizuka, Y. (1999) Cross-reaction of chalcone synthase and stilbene synthase overexpressed in *Escherichia coli*. FEBS Lett. **460**, 457–461
16 Ke, S.-H. and Madison, E. L. (1997) Rapid and efficient site-directed mutagenesis by single-tube 'megaprimer' PCR method. Nucleic Acids Res. **25**, 3371–3372

17 Bradford, M. M. (1976) A rapid and sensitive method for the quantitation of microgram quantities of protein utilizing the principle of protein-dye binding. Anal. Biochem. **72**, 248–254
18 Hrazdina, G., Kreuzaler, F., Hahlbrock, K. and Grisebach, H. (1976) Substrate specificity of flavanone synthase from cell suspension cultures of parsley and structure of release products *in vitro*. Arch. Biochem. Biophys. **175**, 392–399
19 Kreuzaler, F., Light, R. J. and Hahlbrock, K. (1978) Flavanone synthase catalyzes CO_2 exchange and decarboxylation of malonyl-CoA. FEBS Lett. **94**, 175–178
20 Preisig-Muller, R., Gehlert, R., Melchior, F., Stietz, U. and Kindl, H. (1997) Plant polyketide synthases leading to stilbenoids have a domain catalyzing malonyl-CoA:CO_2 exchange, malonyl-CoA decarboxylation, and covalent enzyme modification and a site for chain lengthening. Biochemistry **36**, 8349–8358
21 Schöppner, A. and Kindl, H. (1984) Purification and properties of a stilbene synthase from induced cell suspension cultures of peanut. J. Biol. Chem. **259**, 6806–6811
22 Broun, P., Shanklin, J., Whittle, E. and Somerville, C. (1998) Catalytic plasticity of fatty acid modification enzymes underlying chemical diversity of plant lipids. Science **282**, 1315–1317
23 Hornung, E., Walther, M., Kuhn, H. and Feussner, I. (1999) Conversion of cucumber linoleate 13-lipoxygenase to a 9-lipoxygenating species by site-directed mutagenesis. Proc. Natl. Acad. Sci. U.S.A. **96**, 4192–4197
24 Kreuzaler, F., Ragg, H., Heller, W., Tesch, R., Witt, I., Hammer, D. and Hahlbrock, K. (1979) Flavanone synthase from *Petroselinum hortense*. Molecular weight, subunit composition, size messenger RNA, and absence of pantetheinyl residue. Eur. J. Biochem. **99**, 89–96

Received 21 February 2000/5 May 2000; accepted 13 June 2000